A 20-Year Analysis of Disturbance-Driven Rainfall on O'ahu, Hawai'i

RYAN J. LONGMAN,[a] OLIVER ELISON TIMM,[b] THOMAS W. GIAMBELLUCA,[c,d] AND LAUREN KAISER[e]

[a] *East-West Center, Honolulu, Hawaii*
[b] *Department of Atmospheric and Environmental Sciences, University at Albany, State University of New York, Albany, New York*
[c] *Water Resource Research Center, University of Hawai'i at Mānoa, Honolulu, Hawaii*
[d] *Department of Geography and Environment, University of Hawai'i at Mānoa, Honolulu, Hawaii*
[e] *Hawai'i Cooperative Studies Unit, Honolulu, Hawaii*

(Manuscript received 2 September 2020, in final form 15 March 2021)

ABSTRACT: Undisturbed trade-wind conditions compose the most prevalent synoptic weather pattern in Hawai'i and produce a distinct pattern of orographic rainfall. Significant total rainfall contributions and extreme events are linked to four types of atmospheric disturbances: cold fronts, kona lows, upper-tropospheric disturbances, and tropical cyclones. In this study, a 20-yr (1990–2010) categorical disturbance time series is compiled and analyzed in relation to daily rainfall over the same period. The primary objective of this research is to determine how disturbances contribute to total wet-season rainfall on the Island of O'ahu, Hawai'i. On average, 41% of wet-seasonal rainfall occurs on disturbance days. A total of 17% of seasonal rainfall can be directly attributed to disturbances (after a background signal is removed) and as much as 48% in a single season. The intensity of disturbance rainfall (mm day^{-1}) is a stronger predictor ($r^2 = 0.49$; $p < 0.001$) of the total seasonal rainfall than the frequency of occurrence ($r^2 = 0.11$; $p = 0.153$). Cold fronts are the most common disturbance type; however, the rainfall associated with fronts that cross the island is significantly higher than rainfall produced from noncrossing fronts. In fact, noncrossing fronts produce significantly less rainfall than under mean nondisturbance conditions 76% of the time. While the combined influence of atmospheric disturbances can account for almost one-half of the rainfall received during the wet season, the primary factor in determining a relatively wet or dry season/year on O'ahu is the frequency and rainfall intensity of kona low events.

SIGNIFICANCE STATEMENT: Large-scale weather events have the potential to bring much needed rainfall to dry areas on the Island of O'ahu, but the magnitude of these contributions is not well understood. Here, we examine the daily rainfall attributed to four unique weather event types and compare it with rainfall typically received under normal conditions. On average, net-rainfall contributions from weather events account for 17% of the total wet-season rainfall but can account for as much as 48% of total rainfall in a single season. Cold fronts are the most common type of weather event, but we found that fronts that approach but do not cross the island can have an island-wide drying effect. Understanding the rainfall contributions from each unique weather event type is important in the context of water management and planning.

KEYWORDS: Mesoscale processes; Synoptic climatology; Cold fronts; Rainfall; Mesoscale processes; Extratropical cyclones; Subtropical cyclones; Tropical cyclones

1. Introduction

Set within a region where mean annual open-ocean rainfall is less than 600 mm (Kidd and McGregor 2007), the mountainous terrain of the main Hawai'ian Islands is characterized by extreme spatial rainfall gradients that can exceed 1000 mm annually (Giambelluca et al. 2013). Desert-like precipitation-minimum zones and extreme wet conditions can be found within a few tens of kilometers distance on most of the major islands (Giambelluca et al. 2013). Trade-wind-driven orographic lifting is a major factor of rainfall throughout the year in Hawai'i. On the windward side of each island, trade winds push moist air up the eastern slopes, cooling it to the dewpoint temperature, causing water vapor to condense and form clouds. Trade winds are present 85%–95% of the time in summer and 50%–80% in winter (Sanderson 1993; Garza et al. 2012), making trade-wind orographic rainfall the most prevalent rainfall pattern in Hawai'i. Throughout the year and especially during the Hawai'ian wet season (November–April), the trade-wind regime is frequently interrupted by low pressure systems that bring significant rainfall to the dry leeward sides of the islands. The heaviest year-round rainfall events in Hawai'i have been linked to four types of atmospheric disturbances: cold fronts, kona lows, upper-tropospheric disturbances (upper-level lows), and tropical cyclones (Kodama and Barnes 1997; Caruso and Businger 2006).

Previous studies have focused on the connection between atmospheric disturbances and extreme rainfall at global (e.g., Catto and Pfahl 2013), continental (e.g., Kunkel et al. 2012) and regional (e.g., Ramos et al. 2014) scales. In Hawai'i, preliminary research has focused on defining and mapping spatial patterns of extreme rainfall events (Chu et al. 2009) and on linking extreme rainfall to atmospheric disturbances (Kodama and Barnes 1997; Kaiser 2014). However, little is known about the relative contribution that individual disturbance events have on total wet-season rainfall or if the frequency of these events has changed over time. Kaiser (2014) determined that

Corresponding author: Ryan James Longman, rlongman@hawaii.edu

DOI: 10.1175/MWR-D-20-0287.1

the frequency of both kona low and upper-level low pressure systems has not changed over the past few decades in Hawai'i but little is known about changes in cold-frontal frequency in the region. The influence of cold fronts is of particular importance for the Islands of Kaua'i and O'ahu, which are the most northern of the seven main Hawai'ian Islands and, therefore, the most affected by extratropical systems that migrate into the region from higher latitudes (Chu et al. 2009).

The primary objectives of this research are to 1) classify and quantify the frequency of high impact weather events and study their contributions to rainfall in Hawai'i, 2) detect potential trends in the frequency of these events and explore the how interannual climate variability affects the frequency and intensity of rainfall, and 3) better understand the connection between daily rainfall and synoptic weather types. More specific research tasks are to 1) identify all of the cold fronts, kona lows, upper-level lows and tropical cyclone events that have occurred over 20 consecutive water years between October 1990 and September 2010, 2) analyze the temporal trends in frequency of occurrence of disturbance events, 3) calculate the total water-year (October–September) and wet-season rainfall occurring on disturbance days, 4) calculate the net-rainfall contributions from each disturbance type during the wet season, 5) determine how disturbance frequency and rainfall intensity impact total wet-season rainfall, 6) examine the spatial pattern of rainfall enhancement from each disturbance type, relative to nondisturbance conditions on the Island of O'ahu, and 7) identify linkages between disturbance characteristics and interannual modes of natural climate variability.

2. Background

The climate in Hawai'i is strongly affected by the general atmospheric circulation of the tropical and subtropical Pacific, which is dominated by the descending branch of the Hadley Cell. Near the equator, convective and convergent processes lift air and then push it poleward in the upper troposphere, driving this circulation. In the Northern Hemisphere, air sinks in the subtropics between 20° and 30° latitude and returns to the equator as persistent surface winds from the northeast (trade winds). The strong persistence of the trades, especially during the summer, can be explained by the semipermanent subtropical high pressure ridge that sits northeast of the island chain (Garza et al. 2012). The trade winds move moist air toward the island chain where it is orographically lifted up the mountains providing a consistent source of rainfall along the east-facing slopes (Giambelluca et al. 2013). Typically, clouds from the windward side of the island do not reach the leeward side under normal trade-wind conditions as rainfall diminishes rapidly downwind of the topographic ridge (Scholl et al. 2007). Orographic lifting and subsequent descent of air after crossing a mountain ridge produce a wet windward and dry leeward rainfall pattern on the islands. An exception is the Island of Hawai'i (Big Island), where the flow generates a convergent recirculation, and subsequent orographic rainfall in some leeward areas along the coast (Yang et al. 2008b). In addition, thermally driven local (land–sea) circulation near the coast and along the slopes produce clouds and some precipitation on the leeward sides of the islands, most notably on the Kona Coast and leeward slopes of the Big Island, where a summer maximum of rainfall occurs (Giambelluca et al. 2013; Esteban and Chen 2008; Yang et al. 2008a). High elevations (above ~2100 m) are also dry as a result of the trade-wind inversion, which is present ~79% of the time and limits the vertical development of clouds on the highest mountains (Longman et al. 2015).

Lyons (1982) estimated that 51% of the variance in rainfall in Hawai'i was accounted for by trade-wind-orographic rainfall, 16% by "southwest wind rainfall" (including kona lows and other fall, winter, and spring disturbances), and 6% by convective rainfall. Lyons (1982) also concluded that the southwest wind component was more important for the Islands of Kaua'i, O'ahu, and in drier areas statewide. Kaiser (2014) showed that kona lows contribute from 1% to 25% of the annual wet-season rainfall totals on average for a series of climate stations across Hawai'i with the highest percentage contributions found on the Islands of Kaua'i and O'ahu.

Rainfall in Hawai'i can vary greatly from year to year due to natural modes of climate variability such as the El Niño–Southern Oscillation (ENSO), Pacific–North American (PNA) pattern, the Pacific decadal oscillation (PDO; Diaz and Giambelluca 2012; Frazier et al. 2018), and the North Pacific Oscillation (NPO; Elison Timm et al. 2021). In a recent analysis, Frazier et al. 2018 showed that PNA is the dominant mode affecting wet-season rainfall variability, while ENSO is most significant in the dry season (May–October). Long-term drying trends in both annual and seasonal rainfall have been identified by many recent studies (Chen and Chu 2014; Diaz and Giambelluca 2012; Longman et al. 2015; O'Connor et al. 2015; Frazier and Giambelluca 2017). While it is not clear if the observed drying is related to global climate change (Frazier and Giambelluca 2017), concern has been raised that climate warming might lead to further rainfall reductions in Hawai'i. Recent projections of future rainfall changes in Hawai'i, based on statistical downscaling of CMIP5 global model results (Elison Timm et al. 2015), indicate that the dry areas of the state will see large reductions in wet-season rainfall and wet areas will experience slight increases by the middle of this century for both the medium-low emission scenario (RCP 4.5) and high-emission scenario (RCP 8.5). It should be noted that climate change is also likely to change local moisture-flux convergence with other effects on local rainfall patterns, as shown in pseudoglobal warming downscaling regional model simulations (Zhang et al. 2016).

3. Data and methods

a. Disturbance classification

This section describes the classification methods that were applied to categorize the daily synoptic conditions in the region of the Hawai'ian Islands. The cold-frontal dataset and the detection of crossing and noncrossing fronts are presented in section 3a(1). The classification of upper-level disturbances and kona lows is reviewed in section 3a(2). The tropical

disturbance classification and detection method is introduced in section 3a(3).

1) IDENTIFICATION OF COLD FRONTS

In the subtropical region of Hawai'i, approaching cold fronts can produce heavy rain events in the prefrontal zone with a low-level southerly wind component and/or in the postfrontal zone with a low-level northerly wind component (Kodama and Barnes 1997).

Cold-frontal events are identified in the Hawai'i region from a global dataset of frontal activity (Berry et al. 2011a). The front-detection method follows the techniques of Hewson (1998) and identifies fronts using a thermal-front parameter (Renard and Clarke 1965) based on the gradient of the 850-hPa wet-bulb potential temperature along a moist isentrope (Berry et al. 2011b). Front locations are computed every 6 h for the period spanning 1989–2010 from the ERA-Interim (ERAI) reanalysis (Simmons et al. 2007), which has a 0.5° × 0.5° resolution.

To identify cold-frontal activity in Hawai'i, a set of objective criteria are established at the conclusion of an experimentation period, in which several automated and manual detection methods were explored. The method for cold-frontal detection in the Hawai'i region from the global dataset provided by Berry et al. (2011a) consist of the following set of steps:

1) Cold-frontal coordinates are extracted from the global dataset for the Hawai'i region (17°–26°N, 165°–150°W).
2) A line-joining algorithm is used to link frontal coordinate points into a contiguous front and the points and lines were plotted for each 6-h interval.
3) Images are manually screened to identify the presence of a cold front using the criteria that fronts must:
   i) have at least two contiguous points and
   ii) have a defined path over at least a 12-h period.
4) Images are manually inspected, and frontal events were separated into one of two categories: (i) fronts that cross the island of O'ahu (CR), and (ii) fronts that do not cross the island of O'ahu (NC).
5) For CR events, the ''crossing'' day is identified, and, for the NC events, the day in which the front is at its ''closest'' point to the island of O'ahu was identified. Next, the day prior to and the day after the ''crossing'' day or ''closest'' day are included in the cold-frontal event time series; therefore all CR and NC events consist of a 3-day window, when possible. Note that fronts that stall or dissipate to the west of the island without crossing as well as fronts that make a close pass to the north of the island are included in the NC category. The speed of the cold front was not taken into consideration in the classification.

2) KONA LOW AND UPPER-LEVEL LOW IDENTIFICATION

Previous studies have identified kona lows as large, cold core systems (Simpson 1952) that become cut off from the upper-level westerly winds, creating closed upper-level lows, and subsequently develop a closed surface low (Ramage 1962). Subsequent studies refined this definition, limiting kona lows to systems with centers that form or track south of 30°N (Atkinson 1971; Caruso and Businger 2006). Other studies have further classified kona lows into three categories based on the development of the system, categorizing kona lows as either cold-frontal cyclogenesis, trade wind easterly cyclones, or (combined) cold-frontal cyclogenesis/trade wind easterly cyclones (Otkin and Martin 2004a). In this present work, kona lows (KL) are defined as upper-level lows (UL) that form in the subtropics and are cut off from the midlatitude westerlies over the central North Pacific without the presence of a surface front but with a cyclonic low pressure system at the surface (Caruso and Businger 2006).

Reanalysis of data from the European Centre for Medium-Range Weather Forecasts (ECMWF) interim reanalysis (ERA) project (Dee et al. 2011) was utilized in this study to identify KL and UL events. ERA data are updated in real time at 6-h intervals with 80-km spatial resolution. Using the ERA dataset, two atmospheric levels, 250 hPa and sea level, were analyzed. The potential vorticity field was used as a measure for cyclonic motion at the 250-hPa level, because previous research has shown that the strongest system development occurs at this level (Morrison and Businger 2001). Surface cyclogenesis from upper-level lows was then identified using sea level pressure to classify kona lows. Isobaric contour intervals are displayed at 6-h time intervals from 1990 to 2010, and low pressure systems of interest were identified if they met the following criteria developed by Caruso and Businger (2006):

1) closed cyclonic circulation patterns cut off from the upper-level westerly winds for at least 24 h,
2) tracks south of 30°N,
3) occurrence between 180° and 130°W, and
4) occurrence during October–April.

Following Kaiser (2014), low pressure events are then classified as either UL without surface development or as KL if a closed surface is detected. It is noted that further classification of KL or UL events into western and eastern longitudinal position of the systems relative to the islands or by the dynamic development (Otkin and Martin 2004a,b) could be beneficial in better resolving associations with spatial rainfall patterns. However, it was decided against a finer classification at this point due to a lack of a precedence for well-established classification criteria in scientific literature at the time of the study.

The upper-level lows we consider in this manuscript are lows that are aloft that have not been cut off from the westerlies. These are the upper-level extensions of a low pressure center without surface development can subsequently follow upper-level troughs. We agree that with the reviewer that these types of troughs can create unstable conditions and lead to significant rainfall as do the upper-level lows as indicated in our results at the time of this study.

3) TROPICAL CYCLONE CLASSIFICATION

Tropical cyclones (TC) typically occur during the dry (summer) season and are relatively rare in the study region during the wet season. On average, a tropical cyclone (of tropical depression strength or greater) has been shown to pass within 300 km of the Hawai'ian Islands once every two years (Kodama and Barnes 1997). Landfall by hurricanes are exceptionally rare due

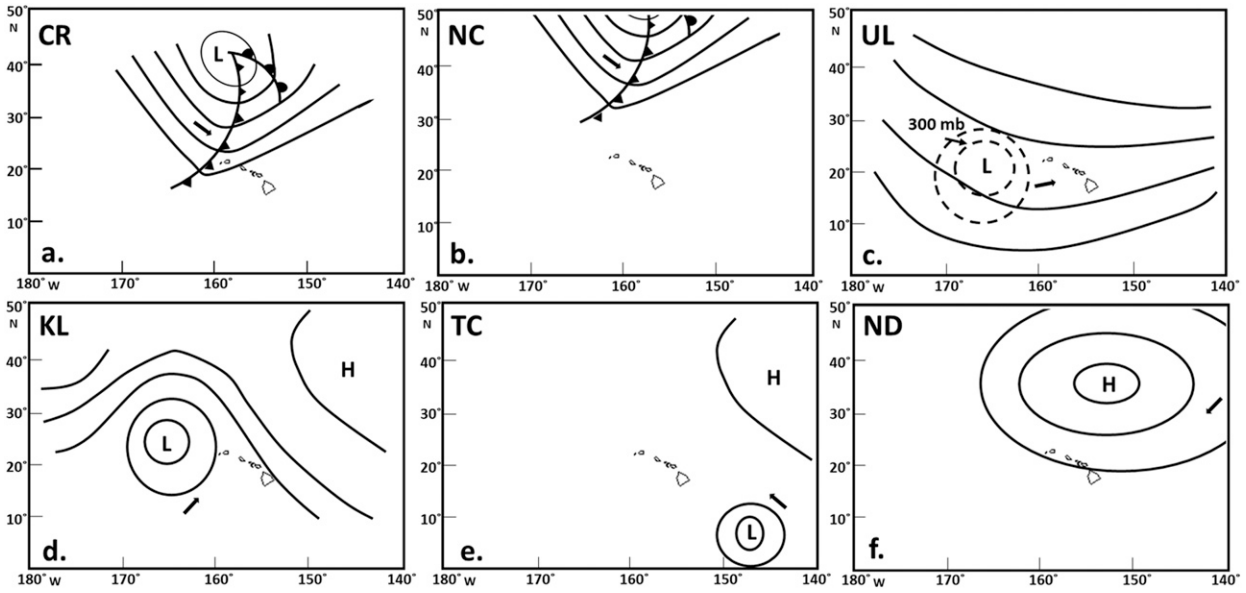

FIG. 1. Schematics showing six types of synoptic patterns that produce rainfall in Hawai'i: (a) crossing fronts (CR), (b) noncrossing fronts (NC), (c) upper-level low pressure systems (UL), (d) kona low storms (KL), (e) tropical cyclones (TC), and (f) nondisturbances (ND). The 500-hPa isobars are indicated with solid black lines and the wind direction is indicated by the arrow.

to several factors including the rather small target that the Hawai'i islands present, the influence of cooler water found to the west of the Island and unfavorable vertical wind shear (Businger et al. 2018). To account for the influence of tropical cyclones on O'ahu rainfall, first, a list of tropical storm tracks is obtained through the National Oceanic and Atmospheric Administration's (NOAA), Central Pacific Hurricane Center. The distances from the center of O'ahu to all points in the individual storm tracks are calculated. Then, for all days during which a TC is within 700 km of the Island, rainfall for that day is assigned to the TC category. The 700-km threshold is chosen based on a recent analysis in which a category-4 hurricane tracking 560 km south of Hawai'i Island was shown to bring island-wide rainfall associated with the storm (Nugent et al. 2020). We consider a 700-km threshold to be a conservative estimate based on the results of this known hurricane event. In addition to using it for storm track identification, the NOAA Technical Memo archive on storm events is also referenced to determine if any individual storm events brought rainfall to O'ahu beyond official storm dissipation date as a result of remnant tropical system moisture advected into the region.

4) NONDISTURBANCE CLASSIFICATION

Nondisturbance days (ND) are considered days in which none of the four disturbance types identified above are present in the daily weather classification time series. The primary rainfall-producing mechanisms on these days are considered to be trade-wind orographic lifting, localized land-sea breeze convective-orographic lifting or convective lifting under weak wind conditions (Hsiao et al. 2020).

A conceptual rendering of the six types of atmospheric disturbances described here is shown in Fig. 1. The conceptual idea for this figure was adapted from the work of Chu et al. (1993), who showed a similar figure describing three of these disturbance types.

b. *Rainfall data and metrics*

Many problems are associated with using individual climate station observations to characterize the extent of island-wide rainfall in Hawai'i. These problems include inconsistencies with the observational records among stations, gaps in individual station records, unequal distribution of stations, and large gaps in the spatial coverage of stations (Longman et al. 2018). One way to overcome these problems is to use a gridded product that makes use of all available observational data. Gridded data can be used to capture an island-wide or smaller-scale spatial pattern by averaging all cells pertaining to a specific area of interest within the grid. In this study, we make use of a 25-yr set of gridded daily rainfall maps for the Island of O'ahu, which were produced at a 250-m resolution (Longman et al. 2019). The rainfall data used to make these maps are derived from a quality controlled and partially gap-filled daily rainfall dataset that included up to 108 unique rainfall stations for O'ahu (see Longman et al. 2018). First, mean daily rainfall is calculated as the average of all the gridded rainfall values for each daily rainfall map. Each day in the time series (1990–2010) is then assigned a single disturbance category (CR, NC, KL, UL, TC, or ND). For days in which the CR or NC event overlapped with a KL or UL event, the CR, or NC event is given priority. This occurred only four times in the time series.

Daily rainfall for each disturbance category is aggregated to both water-year and wet-season averages. In this study, a water year is defined as a 12-month period beginning on 1 October of a given year and ending on 30 September of the following year. For both water-year and wet-season analyses, a year in question is

TABLE 1. Disturbance-event frequency of occurrence for each calendar month that occurred between 1 Oct 1990 and 30 Sep 2010. Category is the disturbance category. Here and in subsequent tables, CR are the cold fronts that cross O'ahu, NC are the noncrossing fronts, KL is the kona low, UL is the upper-level low, and TC is the tropical cyclone. Totals are shown for each disturbance category (last column) and for each calendar month (bottom row); "%" is the percent of disturbances occurring in a given month.

Category	Oct	Nov	Dec	Jan	Feb	Mar	Apr	May	Jun	Jul	Aug	Sep	Total
CR	0	11	29	41	39	22	13	7	0	0	0	0	162
NC	5	13	22	33	23	17	8	3	0	0	0	0	124
KL	10	14	3	4	3	8	2	0	0	0	0	0	44
UL	13	12	8	5	2	3	1	0	0	0	0	0	44
TC	0	0	0	0	0	0	0	0	1	4	9	4	18
Total	28	50	62	83	67	50	24	10	1	4	9	4	392
%	7.1	12.8	15.8	21.2	17.1	12.8	6.1	2.6	0.3	1.0	2.3	1.0	

referenced by the year pertaining to the first month in the time series (e.g., the 1997 wet season runs from 1 November 1997 to 30 April 1998). Data were aggregated in these ways to account for year-to-year variability associated with natural modes of climate variability, such as El Niño–Southern Oscillation (ENSO), which has dramatic effects on weather patterns over consecutive months that often do not fall within the same calendar year.

The percent contributions (Pc) of individual disturbance categories to total rainfall (RF) is calculated for each wet-season and for each water year by taking the sum of the rainfall for each category in a given season or year and dividing it by the total rainfall accounted for in that same season or year [Eq. (1)]. Percent contributions were calculated as the average of 20 complete water years and wet seasons that occurred between 1990 and 2010:

$$\mathrm{Pc} = \left[(\widehat{\mathrm{RF}_{d,i}} \times N_{d,i}) / \sum \mathrm{RF}_i\right] \times 100, \qquad (1)$$

where $\widehat{\mathrm{RF}_{d,i}}$ is the mean daily rainfall for disturbance category d during a season/year (denoted with index i), $N_{d,i}$ is the number of days that events in the disturbance category d were recorded, and $\sum \mathrm{RF}_i$ is the sum of all rainfall from each disturbance type for a given season/year i.

Percent contributions reflect the total amount of rainfall that occurred on individual disturbance days but does not consider that, in the absence of a disturbance, rainfall would likely still occur. To properly quantify the true extent of any additional rainfall contribution or suppression as a result of the presence of an atmospheric disturbance, a ND background signal is subtracted from each disturbance time series to determine the Net Percent contribution (NPc) to wet-season rainfall. To accomplish this, the mean ND daily rainfall for a given year is subtracted from the mean rainfall for each disturbance day during that same year. Rainfall contributions for each season are calculated as the difference between mean disturbance rainfall for each disturbance type and mean ND rainfall, during the same season, multiplied by the number days the disturbance type occurred, and then divided by the total rainfall received that season [Eq. (2)]. Positive values represent the additional rainfall caused by the disturbance and negative values represent the suppression of rainfall due to the presence of a disturbance. Calculating net rainfall this way allows one to determine the relative magnitude of the rainfall contribution or suppression as a result of the disturbance during a season:

$$\mathrm{NPc} = \left\{\left[(\widehat{\mathrm{RF}_{d,i}} - \widehat{\mathrm{RF}_{\mathrm{ND},i}}) \times N_{d,i}\right] / \sum \mathrm{RF}_i\right\} \times 100, \qquad (2)$$

where $\widehat{\mathrm{RF}_{\mathrm{ND},i}}$ is the mean wet-season nondisturbance rainfall for wet season i.

Net contributions are calculated for each individual year and then years are averaged to identify period of record mean contributions and other statistics.

Rainfall enhancements are defined here as the mean or median net rainfall attributed to each disturbance type relative to the mean or median rainfall received during ND conditions. Rainfall enhancements are calculated at each individual 250-m grid cell to demonstrate how wet-season rainfall from each disturbance is distributed spatially across the island [Eq. (3)]. Net-rainfall enhancement (NRE) was calculated as follows:

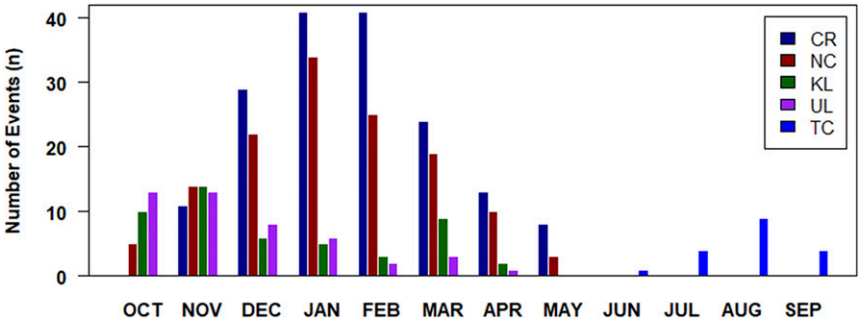

FIG. 2. Frequency of occurrence for each disturbance type from 1 Oct 1990 to 31 Sep 2010.

TABLE 2. Disturbance event frequency of occurrence for water-year and wet seasons occurring between 1990 and 2010. Sum is the total number of disturbance events in the 20-yr time series; Mean is the average number of disturbances per year; SD is the standard deviation of the mean; Max and Min are the maximum and minimum number of disturbances, respectively, occurring in a single year; and "%" is the percentage of occurrences of each disturbance type relative to the total number of disturbances.

	Sum	Mean	SD	Max	Min	%
Water year						
CR	162	8.1	3.9	15	2	41.3
NC	124	6.2	3.3	13	2	31.6
KL	44	2.2	1.7	6	0	11.2
UL	44	2.2	1.4	5	0	11.2
TC	18	0.9	0.9	3	0	4.6
Wet season						
CR	155	7.8	3.6	13	2	46.1
NC	116	5.8	3.1	11	2	34.5
KL	34	1.7	1.3	5	0	10.1
UL	31	1.6	1.3	5	0	9.2
TC	0.0	0.0	0.0	0	0	0.0

$$\mathrm{NRE} = \{([\mathrm{RF}_d] - [\mathrm{RF\_ND}])/[\mathrm{RF\_ND}]\} \times 100, \quad (3)$$

where $[\mathrm{RF}_d]$ is the mean or median rainfall for each disturbance type d and [RF_ND] is mean or median nondisturbance rainfall.

c. *Comparison with interannual modes of climate variability*

The NPc and frequency of occurrence of each disturbance category is compared against PNA and ENSO indices. We used the PNA index (PNAI) calculated by Frazier et al. (2018) who projected the PNA loading pattern onto the daily anomaly 500-hPa height field in the Northern Hemisphere (Chen and van den Dool 2003). The multivariate ENSO index (MEI; Wolter and Timlin 2011) is used to represent the strength and phase of ENSO. This index is derived from six variables over the tropical Pacific: sea level pressure, meridional surface wind, zonal surface wind, surface air temperature, sea surface temperature, and total cloudiness fraction. The MEI has been shown to best represent the atmospheric state associated with ENSO over the Hawai'ian Islands (see Frazier et al. 2018). Monthly values for both indices are averaged for the 6-month wet season and seasonal disturbance characteristics including NPc and event frequency are compared with the two PNAI phases (negative and positive) and three ENSO phases (La Niña, Neutral and El Niño). The Wilcoxon rank-sum test is used to identify significant differences between the median values of each distribution.

d. *Statistical tests*

Linear regression is used to determine if the frequency of occurrence of individual disturbance events changed over time and to compare rainfall contributions received during individual disturbance events with total seasonal rainfall. Rainfall distributions for each individual disturbance type are compared with one another using the nonparametric Mann–Whitney U test (MAN-W) to assess statistical differences between each distribution (one pair at a time). The MAN-W test was selected because the distribution of the rainfall data is determined to be nonnormal. This test is done for wet-season rainfall only; therefore, TC rainfall was not included in this analysis. Significant relationships are evaluated at a threshold of $\alpha = 0.05$. The Wilcoxon rank-sum test was used to identify significant differences in median errors in the seasonal rainfall distributions separated by PNA and ENSO phase described above.

4. Results

a. *Disturbance-event frequency of occurrence*

The number of disturbance events that occurred over the 20 water years in the disturbance time series are identified for each calendar month (Table 1). In total, 392 disturbance events were identified in the time series. The majority of disturbances occurred between October and May, and 86% occur exclusively during the November to April wet season in Hawai'i (as defined in this study) (Fig. 2). January is the most active month for disturbances ($n = 83$) and June is the least active ($n = 1$). Cold-frontal activity (CR and NC) occurred most frequently in January (74 events). Approximately 57% of the fronts are determined to cross the Island of O'ahu and no CR events were identified earlier than November. KL and UL activity occurred between October and April and the maximum activity occurred in November (26 events).

Although not identified in this study, fronts have been reported in the Hawai'i region in both September and June but are considered to be extremely rare (K. Kodama, Senior Service Hydrologist, 2016, personal communication). On 6 September 2017, a weak cold front reached the Islands of Kaua'i, marking the earliest arrival of a cold front to Hawai'i in the 18-yr National Weather Service (NWS) record (NWS/HFO 2017) and in the 30-yr record including the period of this study. The average arrival date of the first cold front as reported by the NWS is 19 October (NWS/HFO 2017).

Frontal activity (CR and NC) represented 73% of the disturbance time series with an average of 14 fronts occurring per year (Table 2). The number of fronts in a given year ranged from a minimum of 6 to a maximum of 22 over the study period. CR fronts ranged from 2 to 15 per year with an average of 8 ± 4 per year. An average of two KL and UL events occur each year with a maximum of six and five events, respectively. As expected, TC events are found only to occur in the dry season (May to October) and represented only 5% of the total disturbance time series. August had the most TC events in the time series ($n = 9$), followed by July and September ($n = 4$). TC events are the least common, occurring on average once per year with a minimum of 0 and a maximum of three in a single year. No significant changes (linear trends) are identified in the frequency of occurrence of any of the disturbance types over the 20-yr period-of-record (Fig. 3). This is not surprising considering that the 20-yr study period is typically not a sufficient amount of time to detect

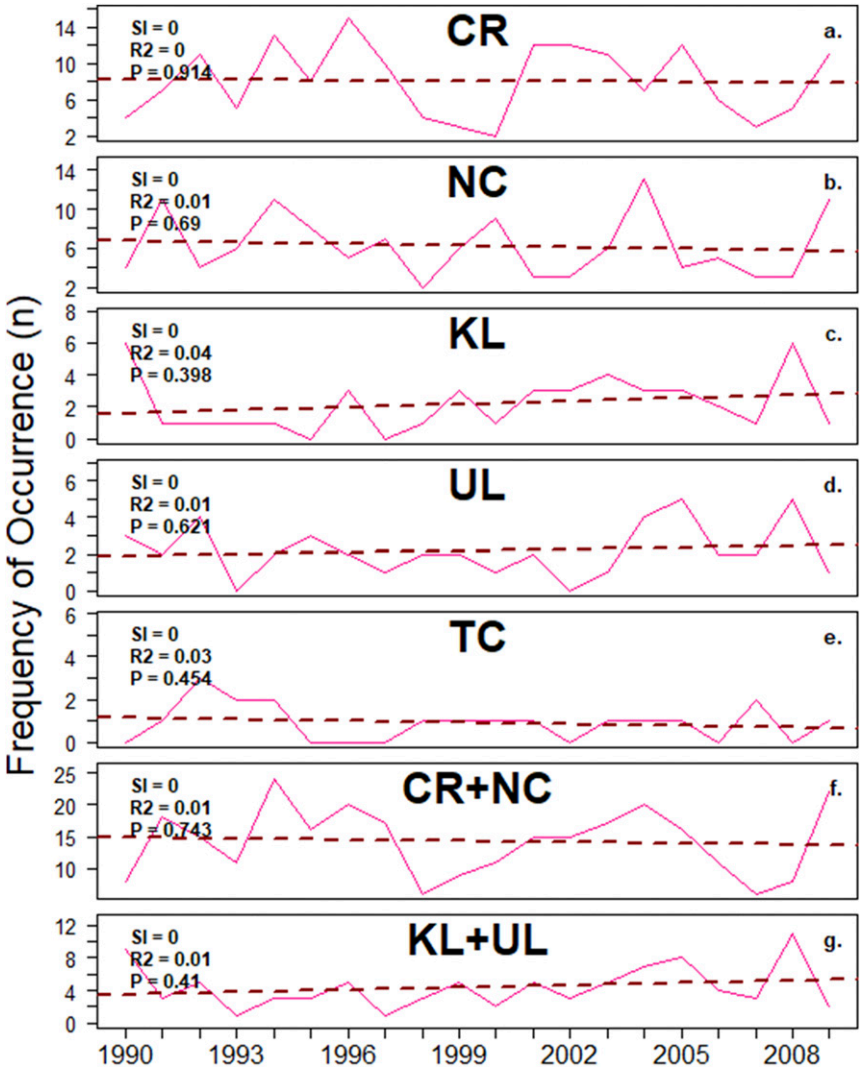

FIG. 3. Disturbance frequency of occurrence for the 20 water years between 1990 and 2010: (a) crossing fronts, (b) noncrossing fronts, (c) kona low storms, (d) upper-level lows, (e) tropical disturbances, (f) the sum of both crossing and noncrossing fronts, and (g) the sum of kona storms and upper-level lows. Here, Sl is the slope of the regression, R2 is the coefficient of determination, and *P* is a measure of significance.

long-term change, especially in Hawai'i where natural modes (e.g., ENSO) are known to cause significant interannual rainfall variability (Frazier et al. 2018).

b. Annual and wet-season disturbance rainfall

On average, ND conditions occur 82% of the time over the year and 70% of the time during the wet season and account for 71% and 59% of the rainfall, respectively (Table 3; Fig. 4). Annually, CR events accounted for 7% of days and are responsible for 12% of the rainfall. NC events account for 4% of the days and 4% of the rainfall. KL and UL events each account for a 3% of the days, and 9% and 4% of the annual rainfall, respectively. During the wet season, CR events accounted for 13% of the days and 19% of the rainfall. NC events account for 7% of the rainfall and KL and UL days accounted 12% and 4% of wet-season rainfall, respectively. TC events account for just 1.6% of annual rainfall and do not occur during the wet season. Mean daily rainfall is greater for CR, KL UL and TC disturbance events relative to mean daily ND rainfall. Mean NC rainfall (3.3 mm day^{-1}) is lower than mean ND rainfall (3.8 mm day^{-1}) for both the water-year and the wet season.

Daily wet-season rainfall distributions associated with each disturbance category are plotted in Fig. 5. Mean and median daily rainfall were highest for KL events, followed by CR, and UL events. Results of the MAN-W test show statistically significant differences for all but one of the pairwise comparisons. Median KL daily rainfall (4.9 mm day^{-1}) was significantly ($p <$

TABLE 3. Mean annual characteristics for rainfall occurring on disturbance days for water-year and wet seasons occurring between 1990 and 2010. Here, ND is nondisturbance, RF mean is the average daily RF for each disturbance type, Days are the average sum (n) or percent (%) of disturbance days in the record, and total RF (%) is the percent of the rainfall occurring on disturbance days.

	RF mean (mm day^{-1})	Days (n)	Days (%)	Total RF (%)
Water year				
CR	6.6	25.5	7.0	11.5
NC	3.1	16.1	4.4	4.0
KL	9.8	11.0	3.0	8.8
UL	4.7	9.9	2.7	3.6
TC	7.1	2.3	0.6	1.6
ND	3.2	300.6	82.4	70.6
Wet season				
CR	6.7	24.4	13.4	18.9
NC	3.3	14.9	8.2	6.7
KL	10.5	8.5	4.7	11.9
UL	3.6	6.9	3.8	3.5
TC	0	0	0.0	0.0
ND	3.8	126.7	69.9	59.0

0.05) greater than all other category medians. CR median rainfall (3 mm day^{-1}) was significantly greater than median NC rainfall (1.1 mm day^{-1}) and median ND (1.6 mm day^{-1}) rainfall. No significant difference was found between mean CR and UL daily rainfall. Results also show the median ND rainfall (1.6 mm day^{-1}) was significantly higher than the median NC rainfall (1.1 mm day^{-1}) suggesting that, a noncrossing frontal event will produce rainfall less than would be received under ND conditions at least half of the time.

c. *Interannual disturbance rainfall variability*

Rainfall occurring on disturbance days accounted for an average 41% of the total seasonal rainfall but varied considerably from year to year (range 11%–69%; Table 4). During the ''wettest'' wet season in the record (2003/04) mean daily rainfall was 8.1 mm and rainfall occurring on disturbance days accounted for 68.5% of the total during that season (Fig. 6). Cold fronts (CR and NC) and KL events accounted 28% and 40% of the total rainfall, respectively, during that season. The ''driest'' wet season in the record, which occurred during the El Niño year of 1997–98, had mean daily rainfall of 2.6 mm, and rainfall on disturbance days accounted for only 32% of the total rainfall that season. No KL events were observed that season and CR and NC events accounted for 28% of the total rainfall. It should be noted, that very low average rainfall on ND days (2.4 mm) was partly responsible for the extreme dryness in that year. Other relatively dry years, for example 1993/94 and 1998/99, had low rainfall contributions from disturbances (11.3% and 16.9%, respectively), but relatively high rainfall on ND days (5.8 and 3.4 mm, respectively).

d. *Net percent contribution (NPc)*

The NPc [Eq. (2)] provides an estimate of how disturbance events influence island-wide rainfall. Since the NPc is a deviation from the mean rainfall received under nondisturbance

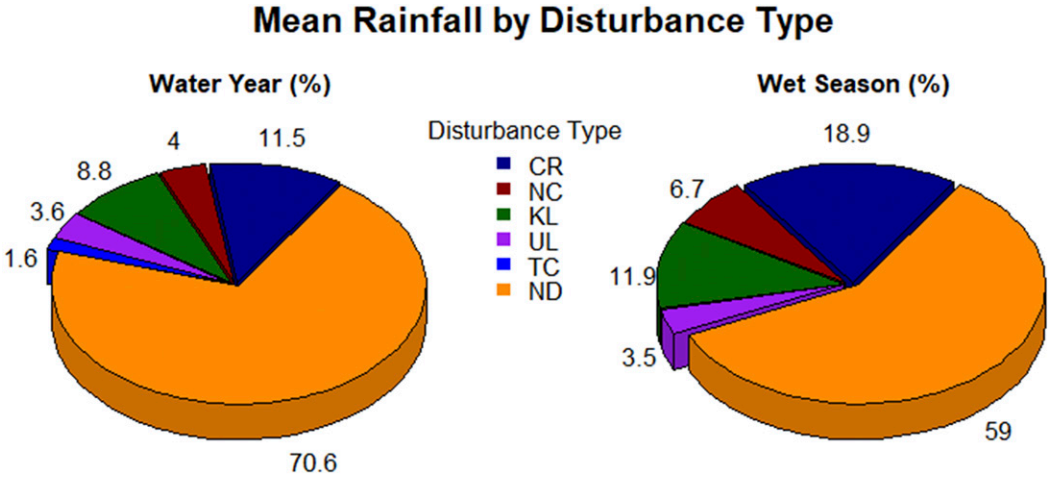

FIG. 4. Percentage of rainfall that has occurred for each disturbance category over (left) the 20 water years and (right) wet seasons that have occurred between 1990 and 2010.

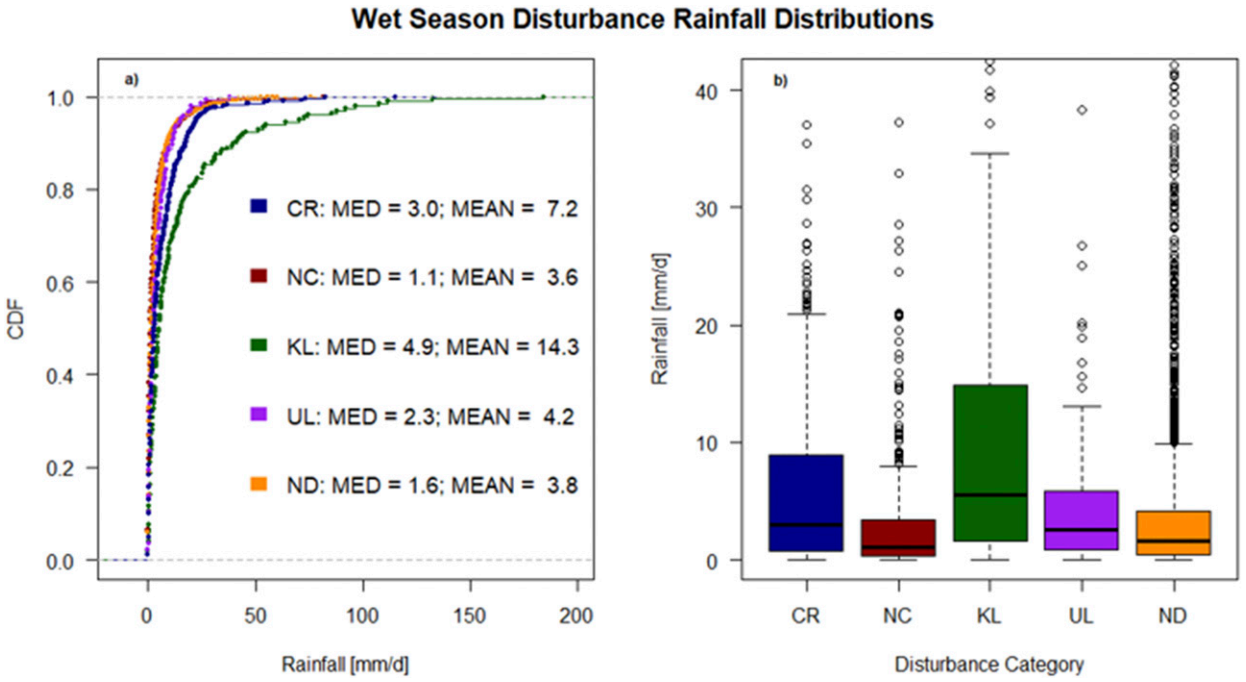

FIG. 5. (a) Wet-season cumulative distribution function and (b) boxplot for daily RF < 42 mm. MED and MEAN are the median and mean rainfall, respectively, in the distributions.

conditions it can be positive or negative. On average, disturbance events account for +17% of the wet-season rainfall beyond what could have been realized under undisturbed trade-wind conditions (range from −8% to +48%; Table 5). On average, CR and KL events account +8% (range from 0 to +37%) and 8% (range from −2% to +33%) of the rainfall received in a single season, respectively. During the 1996/97 wet season, the CR and KL events are attributed to a

TABLE 4. Total rainfall and percent contributions of rainfall for each disturbance type and for each wet season in the record. Total RF is the total island-wide rainfall occurring during a given wet season.

Wet season	Total RF (mm)	CR (mm)	CR (%)	NC (mm)	NC (%)	KL (mm)	KL (%)	UL (mm)	(UL (%)	All (mm)	All (%)
1990/91	1376	103.0	7.5	4.6	0.3	399.7	29.0	3.6	0.3	511.0	37.1
1991/92	530	138.9	26.2	40.7	7.7	2.1	0.4	0.0	0.0	181.7	34.3
1992/93	738	179.4	24.3	15.2	2.1	0.0	0.0	69.1	9.4	263.7	35.8
1993/94	930	40.2	4.3	50.5	5.4	14.4	1.6	0.0	0.0	105.2	11.3
1994/95	626	194.8	31.1	89.7	14.3	10.7	1.7	22.9	3.7	318.1	50.8
1995/96	787	201.2	25.6	48.8	6.2	0.0	0.0	48.1	6.1	298.2	37.9
1996/97	1462	722.5	49.4	83.5	5.7	163.7	11.2	19.5	1.3	989.2	67.7
1997/98	464	68.5	14.8	63.1	13.6	0.0	0.0	16.7	3.6	148.3	32.0
1998/99	690	83.9	12.2	20.7	3.0	6.0	0.9	5.8	0.8	116.4	16.9
1999/2000	669	122.1	18.2	21.2	3.2	15.3	2.3	34.0	5.1	192.6	28.8
2000/01	520	47.2	9.1	17.2	3.3	11.3	2.2	25.5	4.9	101.3	19.5
2001/02	848	137.8	16.2	17.8	2.1	202.2	23.8	38.0	4.5	395.8	46.7
2002/03	590	166.4	28.2	47.6	8.1	82.0	13.9	0.0	0.0	295.9	50.2
2003/04	1465	306.9	20.9	108.8	7.4	583.9	39.9	4.2	0.3	1003.8	68.5
2004/05	1006	127.6	12.7	258.2	25.7	71.3	7.1	101.3	10.1	558.5	55.5
2005/06	1189	175.7	14.8	40.2	3.4	327.1	27.5	72.5	6.1	615.5	51.8
2006/07	615	103.3	16.8	46.1	7.5	41.2	6.7	9.2	1.5	199.9	32.5
2007/08	864	92.7	10.7	9.8	1.1	182.5	21.1	26.5	3.1	311.5	36.1
2008/09	1055	146.7	13.9	1.6	0.2	439.7	41.7	54.0	5.1	642.0	60.8
2009/10	651	135.5	20.8	89.6	13.8	43.0	6.6	26.9	4.1	294.9	45.3
Mean	853.9	164.7	18.9	53.7	6.7	129.8	11.9	28.9	3.5	377.2	41.0
SD	313.4	144.7	10.2	57.2	6.2	174.9	13.7	28.0	3.0	267.5	15.8
Median	762.5	136.6	16.5	43.4	5.6	42.1	6.6	24.2	3.6	297.0	37.5
Min	463.8	40.2	4.3	1.6	0.2	0.0	0.0	0.0	0.0	101.3	11.3
Max	1465.2	722.5	49.4	258.2	25.7	583.9	41.7	101.3	10.1	1003.8	68.5

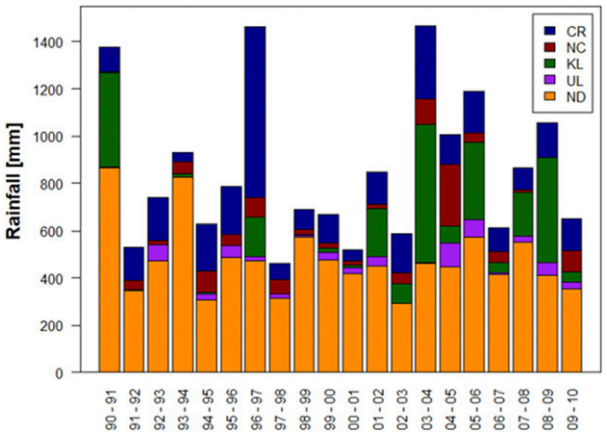

FIG. 6. Total rainfall associated with each disturbance category for wet seasons that occurred between 1990 and 2010.

combined +46% net contribution to total rainfall that season. Net contributions for NC rainfall were less than mean ND conditions for 12 of the 20 years analyzed with a mean contribution of −0.4% (range from −8% to +10%). For some years KL and UL events also showed negative contributions; however, the mean contributions were positive for both disturbance types (+8% and +0.4% respectively). Negative rainfall contributions are most likely explained by a reduction in wind speed that often happens with a disturbance interrupts or reduces trade-wind flow.

To further quantify the importance of disturbance events to the interannual rainfall variability, linear regression analysis was conducted to assess relationships between mean daily wet-season rainfall and the net-rainfall contributions from each disturbance type (Fig. 7). A significant relationship was found when "All" disturbance rainfall contributions were compared with mean daily rainfall ($r^2 = 0.49$; $p = 0.001$). Of the four wet-season disturbance types, kona lows explained the largest fraction of the variability in wet-season rainfall ($r^2 = 0.46$; $p = 0.001$).

e. *Disturbance frequency of occurrence versus wet-season rainfall*

The frequency of occurrence of all disturbance days are not significantly correlated with wet-season rainfall ($r^2 = 0.11$; $p = 0.153$) (Fig. 8). A positive but weak statistical relationship was found between CR activity and mean daily rainfall that was not significant ($r^2 = 0.01$; $p = 0.707$). The frequency of KL events are significantly correlated with wet-season rainfall ($r^2 = 0.48$; $p = 0.001$) and the year with the lowest wet-season rainfall is also one of three years in the period of record in which no KL activity is observed. The two wettest years on record are the years with the greatest number of CR and KL event days. Although not significant, the relationship between NC activity and mean daily rainfall is negative ($r^2 = 0.07$; $p = 0.246$).

f. *Spatial characteristics of disturbance rainfall on O'ahu*

To gain a clear understanding of how disturbance events influence spatial rainfall patterns across the island, daily relative mean and median net-rainfall enhancements are calculated for

TABLE 5. Total rainfall, along with net-rainfall amount and percent contributions of rainfall for each disturbance type and for each wet season in the record.

Wet season	Total RF (mm)	CR (mm)	CR (%)	NC (mm)	NC (%)	KL (mm)	KL (%)	UL (mm)	UL (%)	All (mm)	All (%)
1990/91	1376	103.0	0.6	4.6	−3.3	399.7	20.8	3.6	−1.1	511.0	16.9
1991/92	530	138.9	14.2	40.7	−3.9	2.1	−1.6	0.0	0.0	181.7	8.7
1992/93	738	179.4	8.9	15.2	−1.9	0.0	0.0	69.1	2.9	263.7	9.9
1993/94	930	40.2	0.0	50.5	−6.4	14.4	−1.6	0.0	0.0	105.2	−8.0
1994/95	626	194.8	12.1	89.7	3.2	10.7	−0.6	22.9	1.3	318.1	16.0
1995/96	787	201.2	11.5	48.8	−5.3	0.0	0.0	48.1	−1.2	298.2	5.0
1996/97	1462	722.5	37.3	83.5	2.2	163.7	8.3	19.5	−0.1	989.2	47.7
1997/98	464	68.5	0.0	63.1	4.2	0.0	0.0	16.7	2.1	148.3	6.3
1998/99	690	83.9	5.6	20.7	−0.3	6.0	−1.3	5.8	−2.4	116.4	1.6
1999/2000	669	122.1	12.0	21.2	−4.7	15.3	−2.4	34.0	−0.2	192.6	4.7
2000/01	520	47.2	2.2	17.2	−7.5	11.3	−0.1	25.5	2.1	101.3	−3.4
2001/02	848	137.8	0.8	17.8	−0.9	202.2	20.0	38.0	2.3	395.8	22.2
2002/03	590	166.4	13.6	47.6	4.4	82.0	8.6	0.0	0.0	295.9	26.7
2003/04	1465	306.9	12.6	108.8	4.3	583.9	32.4	4.2	−1.4	1003.8	47.9
2004/05	1006	127.6	3.7	258.2	10.4	71.3	1.7	101.3	2.9	558.5	18.6
2005/06	1189	175.7	3.7	40.2	−1.4	327.1	22.8	72.5	3.3	615.5	28.4
2006/07	615	103.3	8.1	46.1	0.8	41.2	4.8	9.2	−0.9	199.9	12.7
2007/08	864	92.7	7.0	9.8	−1.0	182.5	19.0	26.5	−1.1	311.5	23.9
2008/09	1055	146.7	7.5	1.6	−2.0	439.7	32.5	54.0	−1.9	642.0	36.1
2009/10	651	135.5	5.0	89.6	1.3	43.0	4.7	26.9	2.2	294.9	13.2
Mean	853.9	164.7	8.3	53.7	−0.4	129.8	8.4	28.9	0.4	377.2	16.8
SD	313.4	144.7	8.3	57.2	4.4	174.9	11.7	28.0	1.8	267.5	15.2
Median	762.5	136.6	7.3	43.4	−0.9	42.1	3.2	24.2	0.0	297.0	14.6
Min	463.8	40.2	0.0	1.6	−7.5	0.0	−2.4	0.0	−2.4	101.3	−8.0
Max	1465.2	722.5	37.3	258.2	10.4	583.9	32.5	101.3	3.3	1003.8	47.9

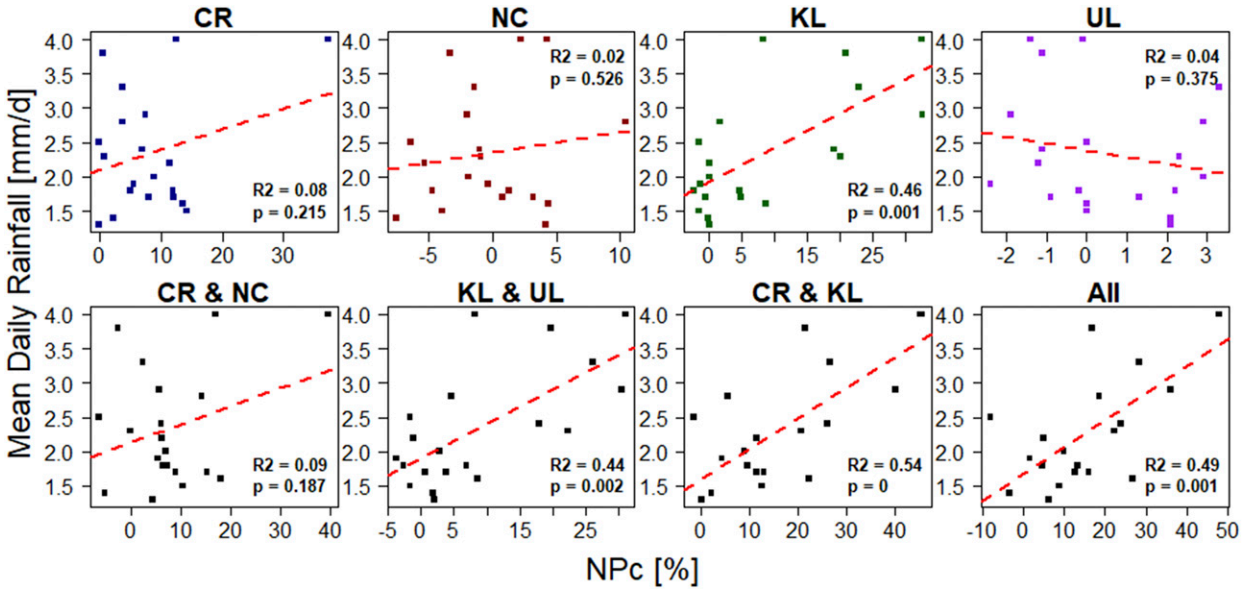

FIG. 7. Mean daily wet-season rainfall compared with disturbance net percent contributions to rainfall. Here, All is all disturbance categories.

each unique disturbance category using the gridded daily rainfall fields (Figs. 9 and 10, respectively). On average, CR and KL events have a positive rainfall enhancement of 88% and 300% beyond what is received under mean ND conditions, respectively. CR and KL mean rainfall enhancement are widespread, with maxima found in the NW and SE parts of the island and minima found leeward of the of the eastern (Koʻolau) mountain range. Median rainfall enhancement for CR and KL days are concentrated at and around the highest point on the Island (Mount Kaʻala; 1227 m) located on the western ridge and along the windward slopes of the eastern range. The SW part of the island and the tips of the SE section (essentially in the driest regions on the island) show very high percentage values for the mean rainfall enhancement and relatively lower values for median rainfall enhancement in those same areas. This indicates that CR and KL events do not always bring rainfall to these parts of the island but can be linked to the more extreme rainfall that occurs in these areas. For NC events, mean rainfall enhancement is positive (8.4%) and most pronounced on the south and west side of the island; however, negative enhancement is observed along the North shore and central interior. Median NC enhancement is negative (−14%) and most pronounced across the

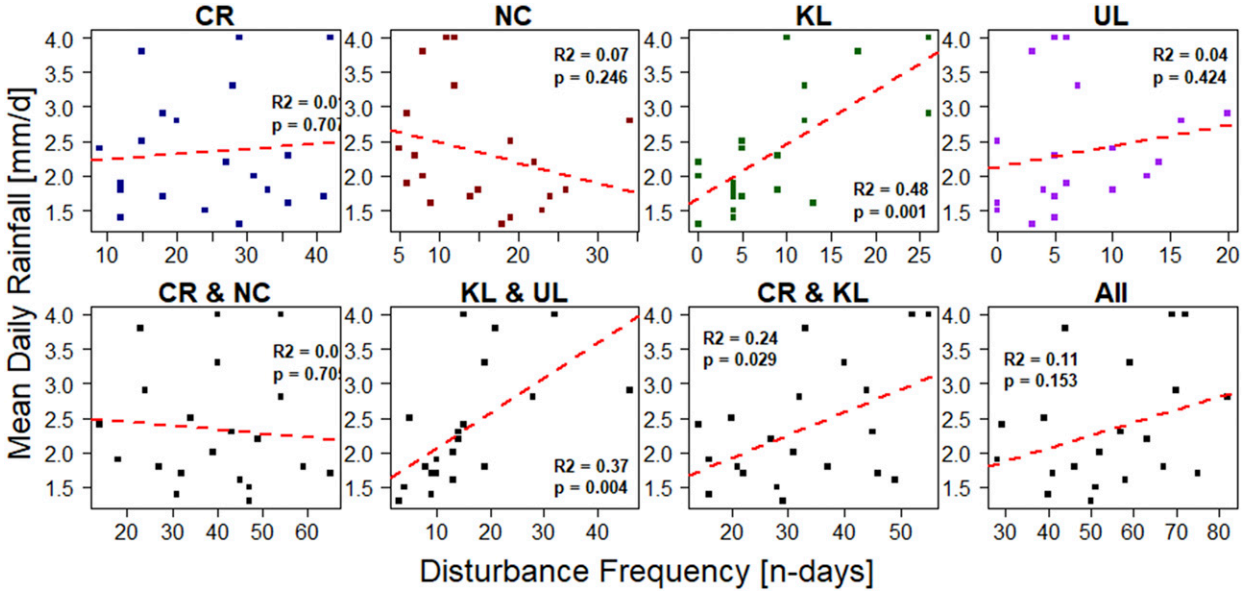

FIG. 8. Mean daily wet-season rainfall compared with the number of disturbance days in a given wet season.

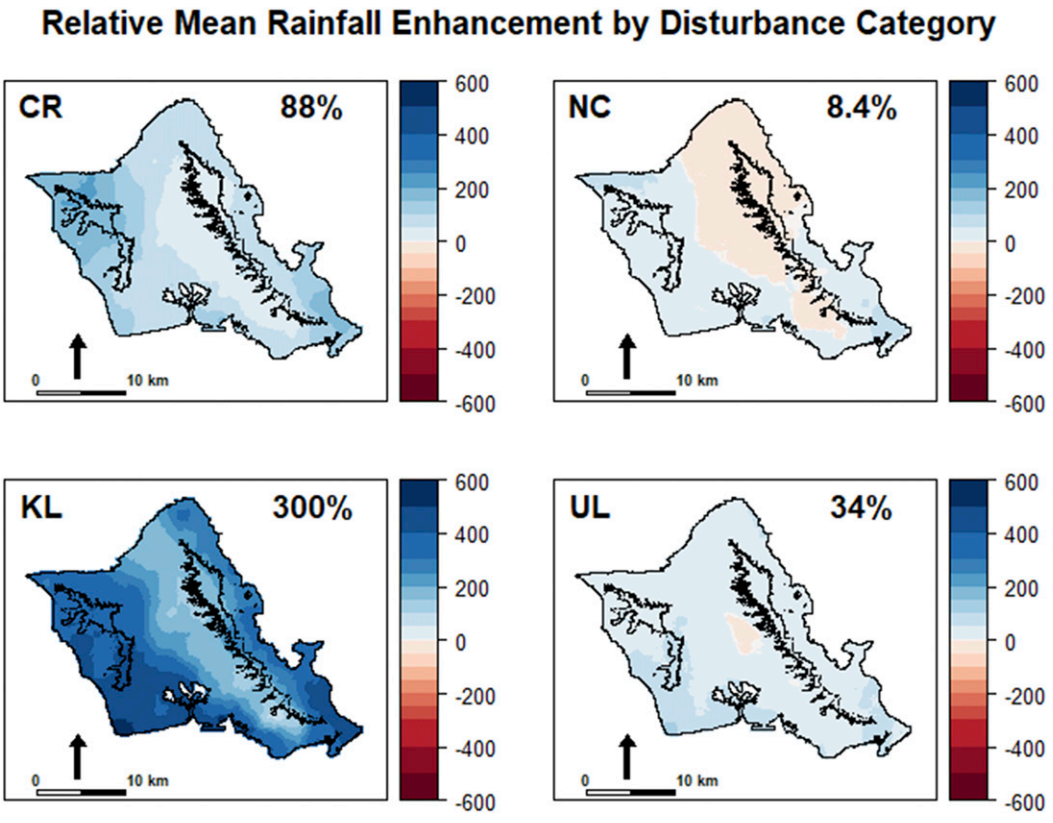

FIG. 9. Mean daily net-rainfall enhancement (%) corresponding to each unique wet-season disturbance category relative to mean nondisturbance conditions. The 500-m elevation contour is shown in black.

northwest mountain range where orographic rainfall is most prevalent, indicating that these types of disturbance events deliver rainfall amounts less than what it typically observed under ND conditions.

g. Noncrossing fronts

The results of the nonparametric statistical test (Table 6) suggest that median NC rainfall is significantly lower than median ND rainfall. To further assess these differences, the daily rainfall for each NC event is compared with the mean daily ND rainfall for the corresponding wet season for all NC occurrences ($n = 300$). Results show that 76% of the time, the NC daily rainfall is less than the mean ND rainfall and the median difference is $-2.2\,\text{mm day}^{-1}$. This suggests that while some NC events have the potential to bring additional rainfall to the islands, most of these events have an island-wide drying effect, relative to what would have occurred during mean ND conditions. The distance of the NC front to the Island did not explain negative NPc. For NC events, a weak correlation was found between distance (closest observable point) from the island and rainfall ($r^2 = 0.013$). Distance relationships were not explored for KL and UL events as a part of this analysis. In general, these findings suggest that some disturbance events (especially NC events) can potentially disrupt trade wind orographic rainfall while not generating frontal lifting over the island sufficient produce rainfall beyond what would have been realized during average ND conditions. The spatial extent of this finding is clearly shown in the NC panels of Figs. 9 and 10, where rainfall enhancement is negative along the windward (eastern) mountain range, which is the area on the island most influenced by orographic trade-wind rainfall.

h. Disturbance characteristics and interannual modes of climate variability

Disturbance characteristics are compared with both PNAI and MEI to determine if these interannual modes of climate variability have a significant effect on either disturbance NPc or frequency of occurrence. In regards to NPc, no significant differences we found (Fig. 11). For the frequency of occurrence, it is determined that significantly more cold fronts (CR and NC) occur during the El Niño phase of ENSO (Fig. 12) when compared with the La Niña phase. Significantly more NC fronts are observed during the positive phase of PNA (but not for CR fronts). The NPc and frequency of occurrence of KL events are low during positive PNA as well as during the El Niño phase.

5. Discussion

Atmospheric disturbances are important sources of rainfall on O‘ahu. On average, disturbances occur on 30% of the days and can account for up to 48% of the total wet-season rainfall. Rainfall produced by cold fronts that cross the Island of O‘ahu

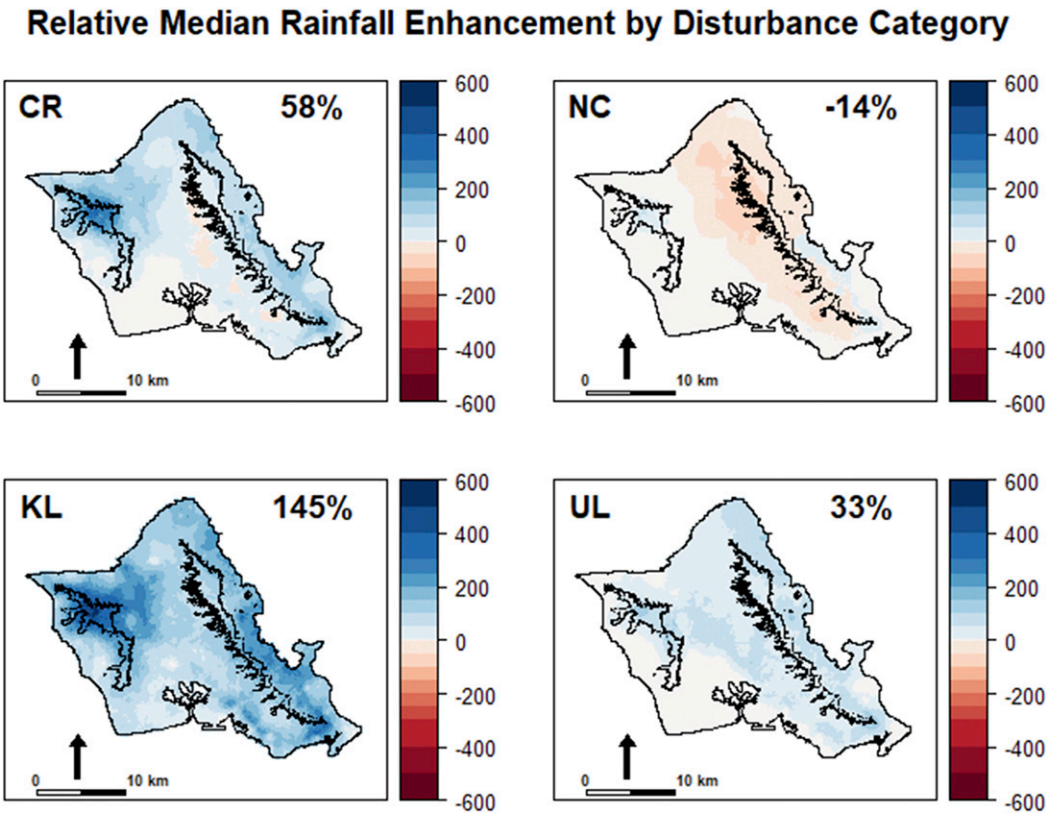

FIG. 10. Median daily net-rainfall enhancement (%) corresponding to each unique wet-season disturbance category relative to median nondisturbance conditions.

are of particular importance because they are the most frequent type of disturbance event and net contributions account for an average 8% and a maximum of 37% of the total wet-season rainfall. The two wettest seasons in the record occur during years with the greatest number of CR and KL event days. During the wettest season in the record (2003/04) net contributions from CR and KL events account for 13% and 32% of the total rainfall, respectively. While CR frequency and rainfall intensity may help to explain "wet years," they are not sufficient predictors of wet-season rainfall variability on their own. In general, the difference between "wet" and "dry" years on the island is predominantly explained by the frequency of KL events and rainfall intensity during KL events.

In this study, disturbance characteristics for each of the unique disturbance types are tested against both a PNA and ENSO index. While, significantly more cold fronts occur during El Niño years, these events are not effective in producing more rain during this phase of ENSO. The fact that crossing fronts increased during El Niño seasons as compared with neutral and La Niña conditions is at first surprising; however, the stronger North Pacific jet supports the passing of disturbances just north of the islands, and according to the data used in this study this includes also crossing fronts. The PNA has been shown to have a stronger influence on Hawai'i's wet-season rainfall (relative to ENSO); however, the causal interrelations between the two modes and how they (independently or concurrently) influence disturbance characteristics is not clearly identified in this study. The median NPc and median frequency of occurrence of KL events is higher during the negative phase of PNA but this result is not significant. The PNAI measures the ENSO-induced circulation teleconnection as well as the internally "weather generated" extratropical variability of the Aleutian low, the strength and position of the subtropical high and storm tracks (Frazier et al. 2018) so this could be an

TABLE 6. Statistical test results for comparisons between rainfall disturbance categories. MAN-W is the nonparametric, Mann–Whitney statistical test; D-MED is the median difference in medians; p value is a measure of statistical significance; and p values in boldface type are $p < 0.05$, which are considered to be significant.

Seasonal category	MAN-W D-MED	MAN-W p value
KL–CR	2.5	**<0.01**
NC–CR	−1.9	**<0.01**
ND–CR	−1.4	**<0.01**
UL–CR	−0.4	0.13
NC–KL	−4.4	**<0.01**
ND–KL	−3.9	**<0.01**
UL–KL	−2.9	**<0.01**
ND–NC	0.5	**0.02**
UL–NC	1.5	**<0.01**
UL–ND	1.0	**<0.01**

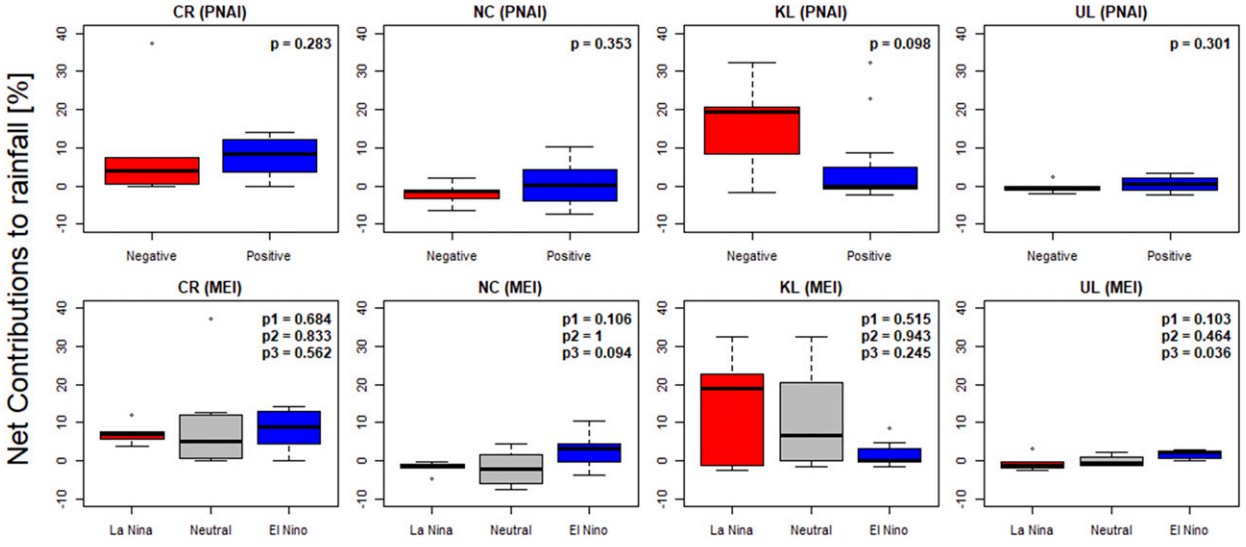

FIG. 11. Net percent rainfall contributions (NPc) for each disturbance type (top) by the Pacific–North America index (PNAI) phase, where negative ($n = 6$) and positive ($n = 14$) are the phases of PNAI, and (bottom) by El Niño–Southern Oscillation phase using the multivariate ENSO index where La Niña ($n = 5$) is the negative phase, El Niño ($n = 7$) is the positive phase, and neutral ($n = 8$) is the intermediate phase of the of the index; p is a measure of statistical significance between the median value of positive and negative phases of PNAI, p1 compares La Niña and El Niño, p2 compares La Niña and neutral, and p3 compares El Niño and neutral phases.

avenue for future research in Hawai'i as additional data become available.

Many environmental changes have been observed over the past decade in Hawai'i. Evidence of long-term decreases in rainfall (Frazier and Giambelluca 2017), decreases in stream and base flow (Bassiouni and Oki 2013), increases in surface air temperature (McKenzie et al. 2019; Kagawa-Viviani and Giambelluca 2020), decreases in dry season cloud cover (Longman et al. 2014), and increases in atmospheric subsidence (Longman et al. 2015). Unequivocally detecting an anthropogenic climate change signal is still difficult for rainfall and hydrological trends in the Hawai'ian Islands (Frazier and Giambelluca 2017). Natural modes of climate variability such as ENSO, PNA, and PDO have been shown to influence the climate of Hawai'i on interannual and interdecadal time scales (Crausbay et al. 2014; Frazier et al. 2018), making detecting trends driven by anthropogenic climate change difficult.

Disturbance characteristics could potentially change as a result of a global warming of Earth's atmosphere. Several studies have projected a decrease in North Pacific storm track activity (less storms) under climate change (O'Gorman 2010; Chang et al. 2012; Lehmann et al. 2014). In addition, simulations also

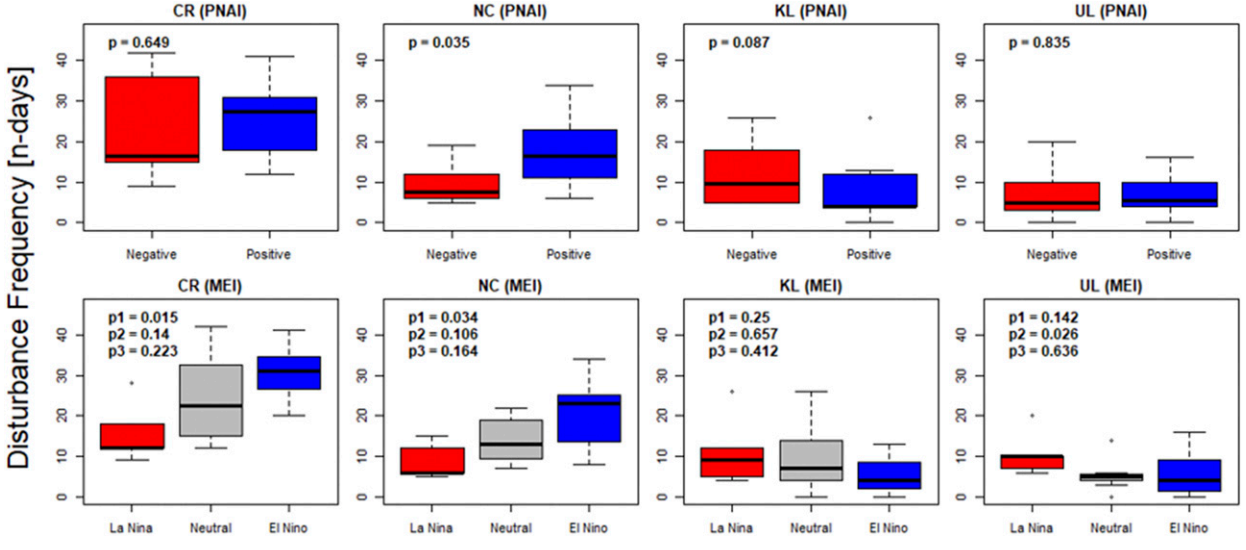

FIG. 12. As in Fig. 11, but frequency of occurrence of each disturbance type is assessed.

show a poleward shift in midlatitude storm tracks during this century as a result of climate change (Yin 2005; Chang et al. 2012) and a corresponding northward shift of associated atmospheric fronts in the Northern Hemisphere (Catto et al. 2011). This suggests that, in the future, cold fronts, UL, and KL events might affect Hawai'i less frequently than at present. However, projected changes in Northern Hemisphere storm tracks are not clear due to the large number of influences that contribute to the response of the storm tracks to a warming climate (Catto et al. 2014). Substantial differences in the projected storm track response to warming are seen between models (Harvey et al. 2012) but the largest consensus exists for a poleward shift in storm tracks in both the Northern and Southern hemispheres (Yin 2005; Chang et al. 2012; Catto et al. 2014).

If storm tracks were to shift poleward, this could potentially reduce the total amount of wet-season rainfall received by cold fronts on O'ahu, as fronts may not track far enough south to cross the island. A significant finding of this study is that the majority of NC events are too far away to produce rainfall on O'ahu, but close enough to disrupt normal trade wind flow, thus limiting orographic rainfall on the island and resulting in net drying effect. An important avenue of future research could be to identify the underlying physical mechanisms that cause some noncrossing fronts to produce high rainfall events and others to have a net drying effect. This could result in a subclassification that improves our overall understanding of the impacts of these noncrossing events. Furthermore, the potential widening of the tropical Hadley circulation (e.g., Chang et al. 2012) cells will be important to study in more detail, since it could affect intensity and frequency of the weather events in the future. Developing a complete understanding of how a poleward shift in storm tracks might influence rainfall in Hawai'i presents another interesting opportunity for future research.

Climate downscaling studies suggest future changes to climate can be expected for the Hawai'ian Islands including increases in temperature, TWI frequency, and TWI strength (Lauer et al. 2013) and decreases in rainfall (Elison Timm et al. 2015). For O'ahu, rainfall is projected to decline by 30% or more in dry (leeward) areas regardless of the season or emission scenario used (Elison Timm et al. 2015). Climate downscaling projections that use a regional climate model (Zhang et al. 2016) and pseudoglobal warming (PGW), projected significant rainfall increases in windward areas and only slight decreases in leeward areas for the CMIP3 SRES A1B scenario for the late twenty-first century. The projections of future climate in Hawai'i from currently available downscaling do not provide a clear consensus how rainfall will change. Uncertainty in statistical downscaling is associated with reliance on the assumed stationarity of the relationships between atmospheric circulation patterns and rainfall (Elison Timm et al. 2015) and might not fully account for changes in disturbance rainfall intensity. On the other hand, PGW simulations do not account for possible future changes in the frequency of disturbances. Combining information on disturbance driven contributions to rainfall with future climate projections is thus a necessary first step toward improving our understanding of variations and long-term changes in rainfall on O'ahu.

Another interesting point of discussion stemming from this work is the characterization of the wet season in Hawai'i. Over the past several decades the wet season has been defined using several different approaches. Besides the 6-month wet-season period running from November to April (as adopted in this work), researchers have also used a 7-month season running from October to April (e.g., Elison Timm et al. 2011), a 5-month season running from November to March (e.g., Chu and Chen 2005) and a 3-month season running from January to March (e.g., Bassiouni and Oki 2013) to characterize the wet season. In all of these instances, researchers point to the wet season as a period in which extratropical atmospheric disturbances, such as low pressure systems, Kona storms, and cold fronts, bring large rainfall events to the Islands, but they do not reference any analysis doe to identify the months when these disturbances occur. The results presented here could provide evidence to support an analysis of the definition of the Hawai'i wet season based on the frequency of occurrence of these disturbances.

6. Conclusions

Atmospheric disturbances can account for almost half of the rainfall received during the wet season; however, the primary factor in determining a relatively wet or dry year on O'ahu are the frequency and rainfall intensity of KL events. Fronts are the most common atmospheric disturbance-types but NC fronts typically produce rainfall less than is received under nondisturbance conditions. Understanding the relative contributions of disturbances to wet-season RF as well as the spatial distribution of RF during these events is important in the context of a changing climate in which disturbances are expected to become less frequent and more intense. Given the importance of these events for the total rainfall on O'ahu, this information can be useful to water managers to plan for changes in water supply and demand in the future, to enable better allocation of resources for developing alternative water sources, to improve water conservation, and to plan for future water-demanding land development. In addition, this research has identified several gaps in our understanding of the underlying physical mechanisms associated with individual disturbance events. We suggest that future research should endeavor to focus on additional subclassifications of both crossing and noncrossing fronts and to identify the role that upper-tropospheric dynamics and thermodynamics has on disturbance driven rainfall in Hawai'i.

Acknowledgments. This research was supported by the Honolulu Board of Water Supply. Additional support for the preparation of this paper came from Hawai'i EPSCoR Program, a National Science Foundation Research Infrastructure Improvement (RII) Track-1: 'Ike Wai: Securing Hawai'i's Water Future Award OIA-1557349 and the Pacific Islands Climate Adaptation Science Center. We sincerely thank Dr. Gareth Berry (University of Leeds) who provided us with the globally gridded cold-frontal dataset. We thank Dr. Andy Newman (National Center for Atmospheric Research), Kevin Kodama (National Weather Service), Mike Nullet (University of Hawai'i), Dr. Abby

Frazier (East-West Center), Barry Usagawa and Nancy Matsumoto (Honolulu Board of Water Supply), and Dr. Robert Scott (Precision Stratigraphy Associates) for supporting various aspects of this work.

Data availability statement. Daily rainfall maps are available online (https://doi.org/10.5065/D6X065VV).

REFERENCES

Atkinson, G. D., 1971: *Forecasters' Guide to Tropical Meteorology*. U.S. Air Force, Air Weather Service, 361 pp.

Bassiouni, M., and D. S. Oki, 2013: Trends and shifts in streamflow in Hawai'i, 1913-2008. *Hydrol. Process.*, **27**, 1484–1500, https://doi.org/10.1002/hyp.9298.

Berry, G., C. Jakob, and M. Reeder, 2011a: Recent global trends in atmospheric fronts. *Geophys. Res. Lett.*, **38**, L21812, https://doi.org/10.1029/2011GL049481.

——, M. J. Reeder, and C. Jakob, 2011b: A global climatology of atmospheric fronts. *Geophys. Res. Lett.*, **38**, L04809, https://doi.org/10.1029/2010GL046451.

Businger, S., M. Puakea, P. W. U. Chinn, and T. Schroeder, 2018: Hurricane with a history: Hawaiian newspapers illuminate an 1871 storm. *Bull. Amer. Meteor. Soc.*, **99**, 137–147, https://doi.org/10.1175/BAMS-D-16-0333.1.

Caruso, S. J., and S. Businger, 2006: Subtropical cyclogenesis over the central North Pacific. *Wea. Forecasting*, **21**, 193–205, https://doi.org/10.1175/WAF914.1.

Catto, J. L., and S. Pfahl, 2013: The importance of fronts for extreme precipitation. *J. Geophys. Res. Atmos.*, **118**, 10 791–10 801, https://doi.org/10.1002/jgrd.50852.

——, L. C. Shaffrey, and K. I. Hodges, 2011: Northern Hemisphere extratropical cyclones in a warming climate in the HiGEM high-resolution climate model. *J. Climate*, **24**, 5336–5352, https://doi.org/10.1175/2011JCLI4181.1.

——, N. Nicholls, C. Jakob, and K. L. Shelton, 2014: Atmospheric fronts in current and future climates. *Geophys. Res. Lett.*, **41**, 7642–7650, https://doi.org/10.1002/2014GL061943.

Chang, E. K. M., Y. Guo, and X. Xia, 2012: CMIP5 multimodel ensemble projection of storm track change under global warming. *J. Geophys. Res.*, **117**, D23118, https://doi.org/10.1029/2012JD018578.

Chen, W. Y., and H. Van den Dool, 2003: Sensitivity of teleconnection patterns to the sign of their primary action center. *Mon. Wea. Rev.*, **131**, 2885–2899, https://doi.org/10.1175/1520-0493(2003)131<2885:SOTPTT>2.0.CO;2.

Chen, Y. R., and P. S. Chu, 2014: Trends in precipitation extremes and return levels in the Hawaiian Islands under a changing climate. *Int. J. Climatol.*, **34**, 3913–3925, https://doi.org/10.1002/joc.3950.

Chu, P. S., and H. Chen, 2005: Interannual and interdecadal rainfall variations in the Hawaiian Islands. *J. Climate*, **18**, 4796–4813, https://doi.org/10.1175/JCLI3578.1.

Chu, P.-S., A. J. Nash, and F.-Y. Porter, 1993: Diagnostic studies of two contrasting rainfall episodes in Hawaii: Dry 1981 and wet 1982. *J. Climate*, **6**, 1457–1462, https://doi.org/10.1175/1520-0442(1993)006<1457:DSOTCR>2.0.CO;2.

Chu, P. S., X. Zhao, Y. Ruan, and M. Grubbs, 2009: Extreme rainfall events in the Hawaiian Islands. *J. Appl. Meteor. Climatol.*, **48**, 502–516, https://doi.org/10.1175/2008JAMC1829.1.

Crausbay, S. D., A. G. Frazier, T. W. Giambelluca, R. J. Longman, and S. C. Hotchkiss, 2014: Moisture status during a strong El Niño explains a tropical montane cloud forest's upper limit. *Oecologia*, **175**, 273–284, https://doi.org/10.1007/s00442-014-2888-8.

Dee, D. P., and Coauthors, 2011: The ERA-Interim reanalysis: Configuration and performance of the data assimilation system. *Quart. J. Roy. Meteor. Soc.*, **137**, 553–597, https://doi.org/10.1002/qj.828.

Diaz, H. F., and T. W. Giambelluca, 2012: Changes in atmospheric circulation patterns associated with high and low rainfall regimes in the Hawaiian Islands region on multiple time scales. *Global Planet. Change*, **98–99**, 97–108, https://doi.org/10.1016/j.gloplacha.2012.08.011.

Elison Timm, O., H. F. Diaz, T. W. Giambelluca, and M. Takahashi, 2011: Projection of changes in the frequency of heavy rain events over Hawaii based on leading Pacific climate modes. *J. Geophys. Res.*, **116**, D04109, https://doi.org/10.1029/2010JD014923.

——, T. W. Giambelluca, and H. F. Diaz, 2015: Statistical downscaling of rainfall changes in Hawai'i based on the CMIP5 global model projections. *J. Geophys. Res. Atmos.*, **120**, 92–112, https://doi.org/10.1002/2014JD022059.

——, ——, S. Li, J. Liu, and D. Beilman, 2021: On the changing relationship between North Pacific climate variability and synoptic activity over the Hawaiian Islands. *Int. J. Climatol.*, **41**, E1566–E1582, https://doi.org/10.1002/joc.6789.

Esteban, M. A., and Y. L. Chen, 2008: The impact of trade wind strength on precipitation over the windward side of the island of Hawaii. *Mon. Wea. Rev.*, **136**, 913–928, https://doi.org/10.1175/2007MWR2059.1.

Frazier, A. G., and T. W. Giambelluca, 2017: Spatial trend analysis of Hawaiian rainfall from 1920 to 2012. *Int. J. Climatol.*, **37**, 2522–2531, https://doi.org/10.1002/joc.4862.

——, O. Elison Timm, T. W. Giambelluca, and H. F. Diaz, 2018: The influence of ENSO, PDO and PNA on secular rainfall variations in Hawai'i. *Climate Dyn.*, **51**, 2127–2140, https://doi.org/10.1007/s00382-017-4003-4.

Garza, J. A., P. S. Chu, C. W. Norton, and T. A. Schroeder, 2012: Changes of the prevailing trade winds over the islands of Hawaii and the North Pacific. *J. Geophys. Res.*, **117**, D11109, https://doi.org/10.1029/2011JD016888.

Giambelluca, T. W., Q. Chen, A. G. Frazier, J. P. Price, Y. L. Chen, P. S. Chu, J. K. Eischeid, and D. M. Delparte, 2013: Online rainfall atlas of Hawai'i. *Bull. Amer. Meteor. Soc.*, **94**, 313–316, https://doi.org/10.1175/BAMS-D-11-00228.1.

Harvey, B. J., L. C. Shaffrey, T. J. Woollings, G. Zappa, and K. I. Hodges, 2012: How large are projected 21st century storm track changes. *Geophys. Res. Lett.*, **39**, L18707, https://doi.org/10.1029/2012GL052873.

Hewson, T. D., 1998: Objective fronts. *Meteor. Appl.*, **5**, 37–65, https://doi.org/10.1017/S1350482798000553.

Hsiao, F., Y.-L. Chen, and D. E. Hitzl, 2020: Heavy rainfall events over central O'ahu under weak wind conditions during seasonal transitions. *Mon. Wea. Rev.*, **148**, 4117–4141, https://doi.org/10.1175/MWR-D-19-0358.1.

Kagawa-Viviani, A. K., and T. W. Giambelluca, 2020: Spatial patterns and trends in surface air temperatures and implied changes in atmospheric moisture across the Hawaiian islands, 1905–2017. *J. Geophys. Res. Atmos.*, **125**, e2019JD031571, https://doi.org/10.1029/2019JD031571.

Kaiser, L. R., 2014: Assessing the impacts of Kona lows on rainfall variability and spatial patterns in the Hawaiian Islands. M.A. thesis, Dept. of Geography, University of Hawai'i at Mānoa, 48 pp, http://hdl.handle.net/10125/101096.

Kidd, C., and G. McGregor, 2007: Observation and characterisation of rainfall over Hawaii and surrounding region from the Tropical Rainfall Measuring Mission. *Int. J. Climatol.*, **27**, 541–553, https://doi.org/10.1002/joc.1414.

Kodama, K., and G. M. Barnes, 1997: Heavy rain events over the south-facing slopes of Hawaii: Attendant conditions. *Wea. Forecasting*, **12**, 347–367, https://doi.org/10.1175/1520-0434(1997)012<0347:HREOTS>2.0.CO;2.

Kunkel, K. E., D. R. Easterling, D. A. R. Kristovich, B. Gleason, L. Stoecker, and R. Smith, 2012: Meteorological causes of the secular variations in observed extreme precipitation events for the conterminous United States. *J. Hydrometeor.*, **13**, 1131–1141, https://doi.org/10.1175/JHM-D-11-0108.1.

Lauer, A., C. Zhang, O. Elison-Timm, Y. Wang, and K. Hamilton, 2013: Downscaling of climate change in the Hawaii region using CMIP5 results: On the choice of the forcing fields. *J. Climate*, **26**, 10 006–10 030, https://doi.org/10.1175/JCLI-D-13-00126.1.

Lehmann, J., D. Coumou, K. Frieler, A. V. Eliseev, and A. Levermann, 2014: Future changes in extratropical storm tracks and baroclinicity under climate change. *Environ. Res. Lett.*, **9**, 084002, https://doi.org/10.1088/1748-9326/9/8/084002.

Longman, R. J., T. W. Giambelluca, R. J. Alliss, and M. L. Barnes, 2014: Temporal solar radiation change at high elevations in Hawai'i. *J. Geophys. Res. Atmos.*, **119**, 6022–6033, https://doi.org/10.1002/2013JD021322.

——, H. F. Diaz, and T. W. Giambelluca, 2015: Sustained increases in lower-tropospheric subsidence over the central tropical North Pacific drive a decline in high-elevation rainfall in Hawaii. *J. Climate*, **28**, 8743–8759, https://doi.org/10.1175/JCLI-D-15-0006.1.

——, ——, and Coauthors, 2018: Compilation of climate data from heterogeneous networks across the Hawaiian Islands. *Sci. Data*, **5**, 180 012, https://doi.org/10.1038/sdata.2018.12.

——, and Coauthors, 2019: High-resolution gridded daily rainfall and temperature for the Hawaiian Islands (1990–2014). *J. Hydrometeor.*, **20**, 489–508, https://doi.org/10.1175/JHM-D-18-0112.1.

Lyons, S. W., 1982: Empirical orthogonal function analysis of Hawaiian rainfall. *J. Appl. Meteor. Climatol.*, **21**, 1713–1729, https://doi.org/10.1175/1520-0450(1982)021<1713:EOFAOH>2.0.CO;2.

McKenzie, M. M., T. W. Giambelluca, and H. F. Diaz, 2019: Temperature trends in Hawai'i: A century of change, 1917–2016. *Int. J. Climatol.*, **39**, 3987–4001, https://doi.org/10.1002/joc.6053.

Morrison, I., and S. Businger, 2001: Synoptic structure and evolution of a kona low. *Wea. Forecasting*, **16**, 81–98, https://doi.org/10.1175/1520-0434(2001)016<0081:SSAEOA>2.0.CO;2.

Nugent, A. D., R. J. Longman, C. Trauernicht, M. P. Lucas, H. F. Diaz, and T. W. Giambelluca, 2020: Fire and rain: The legacy of hurricane lane in Hawai'i. *Bull. Amer. Meteor. Soc.*, **101**, E954–E967, https://doi.org/10.1175/BAMS-D-19-0104.1.

NWS/HFO, 2017: Monthly precipitation summary for the state of Hawaii. NOAA/NWS, Honolulu, HI, accessed 7 February 2017, www.weather.gov/hfo/hydro_summary.

O'Connor, C. F., P. S. Chu, P. C. Hsu, and K. Kodama, 2015: Variability of Hawaiian winter rainfall during La Niña events since 1956. *J. Climate*, **28**, 7809–7823, https://doi.org/10.1175/JCLI-D-14-00638.1.

O'Gorman, P. A., 2010: Understanding the varied response of the extratropical storm tracks to climate change. *Proc. Natl. Acad. Sci. USA*, **107**, 19 176–19 180, https://doi.org/10.1073/pnas.1011547107.

Otkin, J. A., and J. E. Martin, 2004a: A synoptic climatology of the subtropical kona storm. *Mon. Wea. Rev.*, **132**, 1502–1517, https://doi.org/10.1175/1520-0493(2004)132<1502:ASCOTS>2.0.CO;2.

——, and ——, 2004b: The large-scale modulation of subtropical cyclogenesis in the central and eastern Pacific Ocean. *Mon. Wea. Rev.*, **132**, 1813–1828, https://doi.org/10.1175/1520-0493(2004)132<1813:TLMOSC>2.0.CO;2.

Ramage, C. S., 1962: The subtropical cyclone. *J. Geophys. Res.*, **67**, 1401–1411, https://doi.org/10.1029/JZ067i004p01401.

Ramos, A. M., N. Cortesi, and R. M. Trigo, 2014: Circulation weather types and spatial variability of daily precipitation in the Iberian Peninsula. *Front. Earth Sci.*, **2**, 25, https://doi.org/10.3389/feart.2014.00025.

Renard, R. J., and L. C. Clarke, 1965: Experiments in numerical objective frontal analysis. *Mon. Wea. Rev.*, **93**, 547–556, https://doi.org/10.1175/1520-0493(1965)093<0547:EINOFA>2.3.CO;2.

Sanderson, M., 1993: *Prevailing Trade Winds: Climate and Weather in Hawaii*. University of Hawaii Press, 127 pp.

Scholl, M. A., T. W. Giambelluca, S. B. Gingerich, M. A. Nullet, and L. L. Loope, 2007: Cloud water in windward and leeward mountain forests: The stable isotope signature of orographic cloud water. *Water Resour. Res.*, **43**, W12411, https://doi.org/10.1029/2007WR006011.

Simmons, A., and Coauthors, 2007: ERA-Interim: NEW ECMWF reanalysis pro-ducts from 1989 onwards. *ECMWF Newsletter*, No. 110, ECMWF, Reading, United Kingdom, 25–35, https://www.ecmwf.int/node/17713.

Simpson, R. H., 1952: Evolution of the kona storm, a subtropical cyclone. *J. Meteor.*, **9**, 24–35, https://doi.org/10.1175/1520-0469(1952)009<0024:EOTKSA>2.0.CO;2.

Wolter, K., and M. S. Timlin, 2011: El Niño/Southern Oscillation behaviour since 1871 as diagnosed in an extended multivariate ENSO index (MEI.ext). *Int. J. Climatol.*, **31**, 1074–1087, https://doi.org/10.1002/joc.2336.

Yang, Y., Y. L. Chen, and F. M. Fujioka, 2008a: Effects of trade-wind strength and direction on the leeside circulations and rainfall of the island of Hawaii. *Mon. Wea. Rev.*, **136**, 4799–4818, https://doi.org/10.1175/2008MWR2365.1.

——, S. P. Xie, and J. Hafner, 2008b: Cloud patterns lee of Hawaii island: A synthesis of satellite observations and numerical simulation. *J. Geophys. Res.*, **113**, D15126, https://doi.org/10.1029/2008JD009889.

Yin, J. H., 2005: A consistent poleward shift of the storm tracks in simulations of 21st century climate. *Geophys. Res. Lett.*, **32**, L18701, https://doi.org/10.1029/2005GL023684.

Zhang, C., Y. Wang, K. Hamilton, and A. Lauer, 2016: Dynamical downscaling of the climate for the Hawaiian islands. Part II: Projection for the late twenty-first century. *J. Climate*, **29**, 8333–8354, https://doi.org/10.1175/JCLI-D-16-0038.1.